Configurations and level structure of ^{215}Po

C. F. Liang and P. Paris
Centre de Spectrométrie Nucléaire et de Spectrométrie de Masse, Bâtiment 104, F-91405 Campus Orsay, France

R. K. Sheline
Departments of Chemistry and Physics, Florida State University, Tallahassee, Florida 32306
(Received 17 September 1998)

The level structure of ^{215}Po has been studied by observing the alpha decay of ^{219}Rn and coincident gamma rays and electrons. In addition to some new levels, some additional tentative spin and parities are observed. Quite different alpha decay hindrance factors make possible the assignment of $\pi(h_{9/2})^2\nu(g_{9/2})^5$ plus residual reflection asymmetric configurations to one set of states and $\pi(h_{9/2})^2\nu(g_{9/2})^4 i_{11/2}$ plus residual configurations to another set of states. These configuration assignments are further studied by a comparison of the systematics of the ^{215}Po levels with those of neighboring odd neutron nuclei. In this way the nature of the collapse of the reflection asymmetric configurations into the less degenerate shell model configurations can be studied. [S0556-2813(99)03602-X]

PACS number(s): 27.80.+w, 21.60.Cs, 23.20.Lv, 23.60.+e

I. INTRODUCTION

The nuclear region just beyond the reasonably inert ^{208}Pb core can be used as a testing ground of the interplay between independent particle and collective aspects of nuclear structure. This is true because the nuclei in this region, like the nucleus of this study—^{215}Po—have several nucleons, in our case seven, beyond the double closed shell. Thus the appropriate shell model configurations are quite complex. On the other hand, there are not enough valence nucleons to sustain a stable deformed system which could be treated by one of the collective models such as the octupole-quadrupole or the normal Nilsson model.

One of the best ways to understand the interplay of the shell model and collective models in ^{215}Po is to observe the level sequences of a number of neighboring odd-*A* nuclei in the vicinity of ^{215}Po. In this way one can follow individual levels as a function of neutron number and proton number that span the sequences between relatively pure shell model configuration and the quadrupole-octupole collective model [1]. In a similar way one can use the hindrance factors (HF's) of alpha decaying sequences which span the same region to understand the similarities and differences between states.

The level structure of ^{215}Po has been studied on several occasions following alpha decay of ^{219}Rn [2]. In addition the β^- decay of ^{215}Bi [3] is in substantial agreement with the results from alpha decay. These results give a firm foundation on which to base additional experiments. They also give conclusive evidence for J^π values of $9/2^+$, $7/2^+$, and $5/2^+$ for the ground state, 271.23 keV state, and 401.81 keV state, respectively [2]. However, no other spins and parities have been suggested.

In this paper, then, we reinvestigate the levels in ^{215}Po using the alpha decay of ^{219}Rn employing alpha, gamma, and electron spectroscopy in order to understand more completely the spin parities, the configurations, and the relationship of the level structure with neighboring nuclei. Four additional levels and 14 additional gamma transitions have been observed, and in particular the level structure can be understood in terms of specific configurations which are consistent with those of neighboring nuclei.

II. EXPERIMENTAL MEASUREMENTS AND RESULTS

The ^{219}Rn sources (3.96 s) were obtained in our experiment from a massless ^{223}Ra source (11.435 d) of ~ 5 μc. The ^{219}Rn recoils from ^{223}Ra impinged on a transport tape 2 mm away from the ^{223}Ra source. The ^{219}Rn recoils implanted in the tape were moved between alpha, gamma, and electron detectors every 10 s over a period of 2 weeks. During this time we collected approximately 10^5 ^{219}Rn sources. The ^{223}Ra source was obtained from ^{227}Ac (21.8 y) with which it was in secular equilibrium. The preparation of the ^{223}Ra source has been described previously [1].

The alpha detector used in our measurements was an ion implanted Si wafer 200 mm^2 in area and 100 μm thick with 21 keV resolution [full width at half maximum (FWHM)]. The gamma detector was a 20% efficient coaxial Ge detector with a Be window. The source was placed between the alpha and gamma detectors in 180° very close geometry. Singles alpha and gamma spectra were taken together with 512×2048 channels α-γ or α-e$^-$ coincidence measurements. Conversion electrons were detected using a Si(Li) wafer 700 mm^2 in area and 6 mm thick (with 2 keV resolution) placed inside an axially increasing magnetic field. This magnetic lens has a large efficiency (2.3%) and a large energy range (10–600 keV) [4]. The conversion electrons are observed at 90° with respect to the alphas on the same side of the ^{219}Rn source.

Within a second of their preparation the ^{219}Rn sources are in secular equilibrium with ^{215}Po (1.781 ms) and within a few hours it is also in equilibrium with ^{211}Pb (36.1 min), ^{211}Bi (2.14 min), and ^{211}Po (0.516 s). It is therefore difficult to avoid all of the contaminating decay products.

Figure 1 shows that portion of the alpha spectrum of ^{219}Rn which includes the ^{215}Po and ^{211}Bi alpha spectra in secular equilibrium. The three strong ^{219}Rn alpha groups at 6819, 6553, and 6425 keV populate the ground state, 271.23

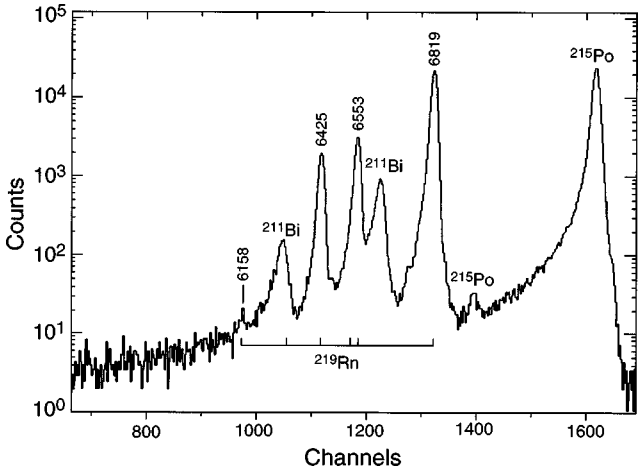

FIG. 1. Alpha spectra of ^{219}Rn, ^{215}Po, and ^{211}Bi. Energies of the alpha groups of ^{219}Rn are given in keV and alpha groups from ^{215}Po and ^{211}Bi are labeled. See text for further discussion of these spectra.

and 401.81 keV states, respectively, in ^{215}Po, while the two strong alpha groups of ^{211}Bi populate the ground state and 351.059 keV state in ^{207}Tl [2]. These five alpha groups of ^{219}Rn and ^{211}Bi dominate the alpha spectrum so severely that it is very difficult to observe the lower energy alpha groups of ^{219}Rn which populate the higher energy states of ^{215}Po. By observing the ^{219}Rn direct spectrum as shown in Fig. 1 for just 1200 s it is possible to see the weak 6158 keV alpha peak (intensity 2×10^{-4}) populating the 676.7 keV level in ^{215}Po. With longer measurements the ^{211}Bi alpha peaks become much larger and observe the ^{219}Rn alpha peak at 6158 keV. Unfortunately the 6311 keV ^{219}Rn alpha peak is masked by the ^{211}Bi alpha peaks. The shapes of the ^{215}Po and ^{211}Bi alpha peaks are broader and have more prominent tails than the ^{219}Rn alpha peaks in Fig. 1 because the ^{215}Po and ^{211}Bi nuclei were implanted into the surface of the alpha detector in the decay of ^{219}Rn. In order to observe the weaker alpha groups of ^{215}Po, all alpha groups in coincidence with gamma rays with energies greater than 401.81 keV are shown in Fig. 2. The emphasis in this paper is placed on the weaker alpha groups populating higher energy states in ^{215}Po since they are most likely to yield new information. Energies and intensities of all alpha groups are given in the ^{215}Po level scheme later in this paper.

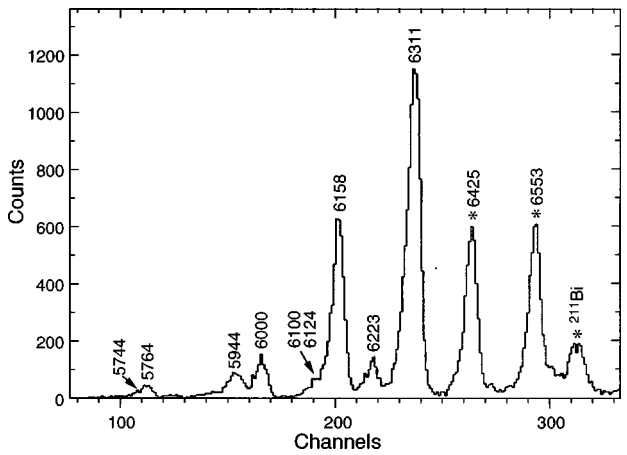

FIG. 2. Alpha spectra of ^{219}Rn and ^{211}Bi in coincidence with all gamma rays greater than 401.81 keV. Energies of the alpha groups of ^{219}Rn are given in keV while ^{211}Bi is labeled. Those groups which are labeled with an asterisk arise because of chance coincidences.

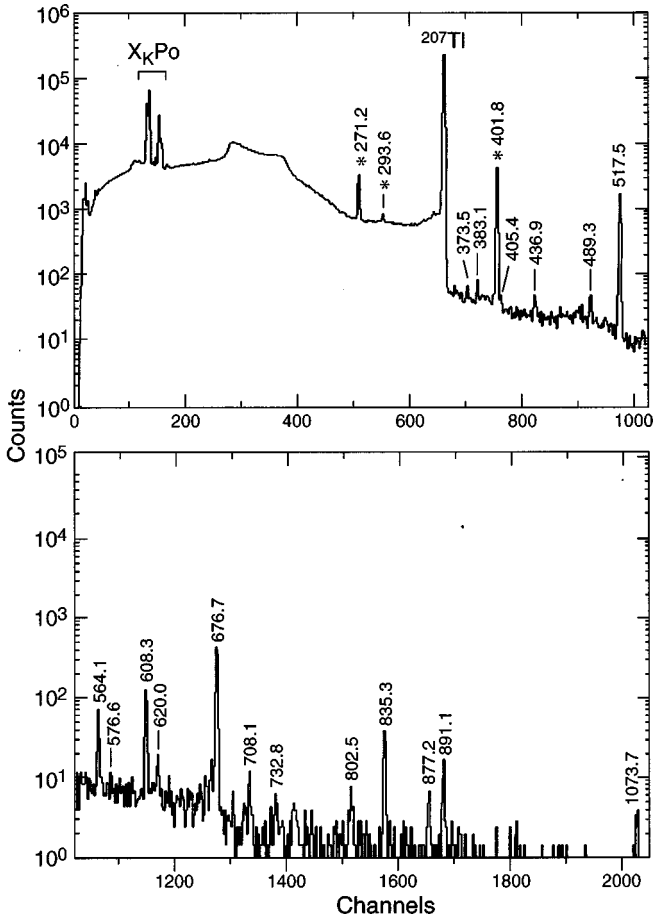

FIG. 3. Gamma rays of ^{215}Po in coincidence with the weak alpha groups of Fig. 2. Coincidences with all alpha groups in the 5700–6350 keV range are shown corresponding to the population of all levels with energies greater than 401.81 keV. Energies of the gamma rays are given in keV. Those gamma rays marked by an asterisk result from the tails of the 6425, 6530, and 6533 keV alphas of ^{219}Rn. The 351.059 keV gamma of ^{207}Tl is also indicated.

Figure 3 shows the gamma spectrum in coincidence with all alpha groups with energies from 5700 to 6350 keV. Those alpha groups populate levels greater than 401.81 keV. All of the energies of the gamma ray transitions in ^{215}Po observed in this study are listed in Table I together with their intensities, their multipolarities when known, and their position in the level scheme.

Internal conversion electrons in coincidence with all alphas of ^{219}Rn and ^{211}Bi are presented in Fig. 4. Using the intensities of the *K*, *L*, and *M* lines, the multipolarities of a number of transitions in ^{215}Po have been determined. They are listed in Table I.

III. LEVEL SCHEME OF ^{215}Po

Using our results in the figures and Table I from Sec. II of this paper, we have constructed the level scheme for ^{215}Po presented in Fig. 5. The energies of the levels and transitions

TABLE I. Gamma ray transitions in ^{215}Po following the alpha decay of ^{219}Rn.

$E\gamma(\Delta E)$	$I\gamma(\Delta I)$[a]	Multipol.	Initial level → final level
130.6(1)	17(2)	$M1+25\%E2$	401.8→271.2
224.0(7)	0.13(2)		517.6→293.6
271.23(5)[b]	1000(20)	$E2+6\%M1$	271.2→0
293.6(1)	6.8(4)	$M1+(E2)$[c]	293.6→0
321.8(10)[d]	0.008(4)		(930)→608.3
330.8(4)[d]	0.090(10)		732.6→401.8
373.5(6)	0.023(3)		891.1→517.6
383.1(6)	0.040(6)		676.7→293.6
401.81(5)	590(20)	$E2$	401.8→0
405.4(6)[d]	0.023(4)		676.7→271.2
436.9(6)	0.028(5)		708.1→271.2
461.6(8)[d]	0.015(3)		732.8→271.2
489.3(5)[d]	0.058(8)		891.1→401.8
517.5(1)	4.0(2)	$M1+(E2)$[c]	517.6→0
556.1(10)[d]	0.005(3)		1073.7→517.6
564.1(3)	0.14(3)		835.3→271.2
576.6(10)[d]	0.008(4)		1094→517.6
608.3(2)	0.40(10)		608.3→0
619.9(6)[d]	0.03(1)		891.1→271.2
665.5(10)[d]	0.008(4)		(959)→293.6
671.9(6)[d]	0.02(1)		1073.7→401.8
676.7(1)	1.6(2)		676.7→0
708.1(8)[d]	0.03(1)		708.1→0
732.8(10)	0.006(3)		732.8→0
802.5(6)[d]	0.03(1)		1073.7→271.2
835.3(3)	0.15(3)		835.3→0
877.2(6)[d]	0.03(1)		877.2→0
891.1(4)	0.07(2)		891.1→0
1073.7(6)[d]	0.03(1)		1073.7→0

[a] $I\gamma/100\alpha = I\gamma \times 0.0108$.
[b] $I\gamma$ normalized on the 271.23 keV transition.
[c] Multipolarity by α_K measurement.
[d] New transition.

are given in keV, and to the right the energies, intensities, and HF's of the alpha groups are given. Since the HF's are important in the discussions of spin parities and configurations in ^{215}Po we outline our method of their determination. We used the ground state to ground state alpha decay of the neighboring even-even nuclei, ^{218}Rn and ^{220}Rn, assuming HF's=1. This allowed us to calculate A and B in the classic formula

$$(\log_{10} T_{1/2})_{\text{theo}} = A + BQ^{-1/2}, \tag{1}$$

using the half-lives and the Q_α's of ^{218}Rn and ^{220}Rn. We then use Eq. (1) to calculate the half-lives for the various alpha groups in ^{219}Rn. The comparison of the observed partial half-lives with the calculated partial half-lives gives us the HF's directly. Tentative spins are put in parentheses and shell model configurations are indicated. The level structure $\leqslant$676.7 keV is in excellent agreement with previous experiment [2]. Above this energy we did not observe the tentative level at 683.7 keV or the level at 1056 keV. On the other hand, we observe new levels at 708.1, 877.2, 1073.7, and 1094 keV, and a tentative level at 930 keV.

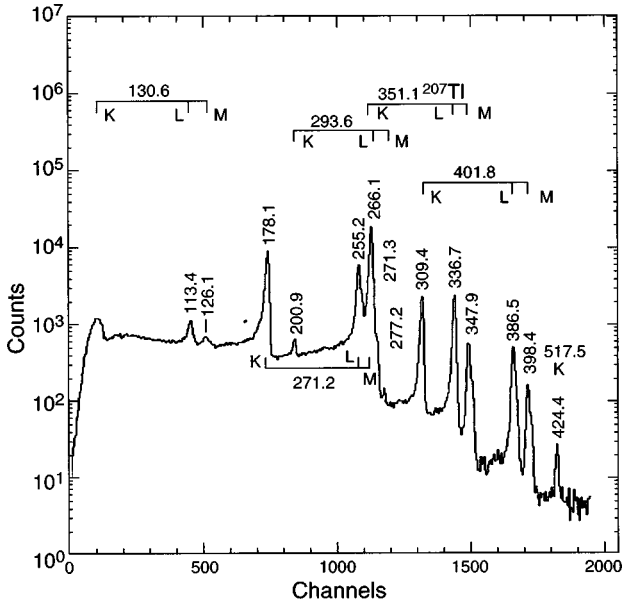

FIG. 4. Internal conversion electron spectrum in coincidence with all alpha groups of ^{219}Rn and ^{211}Bi. Energies of K, L, and M electron lines are given in keV and the corresponding ^{215}Po and ^{207}Tl transition energies in keV are also indicated.

The basis of the 930 keV level was the observation of a weak alpha peak at 5900±15 keV in coincidence with the 608.3 keV gamma ray corresponding to a 935±15 keV level. If one gates on the alpha in this energy range, one observes a weak gamma ray of 321.8 keV which is the connection between the more accurate 930 and 608.3 keV levels. With the possible exception of the 930 keV level, we feel quite confident of the level structure of ^{215}Po in Fig. 5.

It should, however, be stated clearly at the outset of the discussion of the ^{215}Po level scheme that, although the levels connecting transitions (a number with multipolarities) and therefore a number of parities have been clearly established in this experiment, relatively few spins of states have definitely been determined. The ground 271.23 keV, and 401.81 keV states have previously [2] been established as $9/2^+$, $7/2^+$, and $5/2^+$ and our measurements confirm these assignments. Furthermore, these assignments are very useful in making plausibility arguments for the spins of some of the other states. We have attempted to do this, taking into account shell model expectations. However, it must be remembered that, except for the $9/2^+$, $7/2^+$, and $5/2^+$ states, none of the spins of the other states has been determined with certainty, although the states at 293.60 and 517.55 keV have been shown to have positive parity as a result of multipole determinations on some of the transitions.

IV. CONFIGURATIONS IN $^{215}_{84}$Po$_{131}$

We can expect that the ground state configuration of ^{215}Po with two protons and five neutrons beyond the ^{208}Pb double closed shell should be $\pi(h_{9/2})^2\nu(g_{9/2})^5$. Just the neutron part of this configuration would give rise to partial states $1/2^+$, $3/2^+$, $5/2^+$ (twice), $7/2^+$ (twice), $9/2^+$ (3 times), $11/2^+$ (twice), $13/2^+$ (twice), $15/2^+$ (twice), $17/2^+$ (twice),

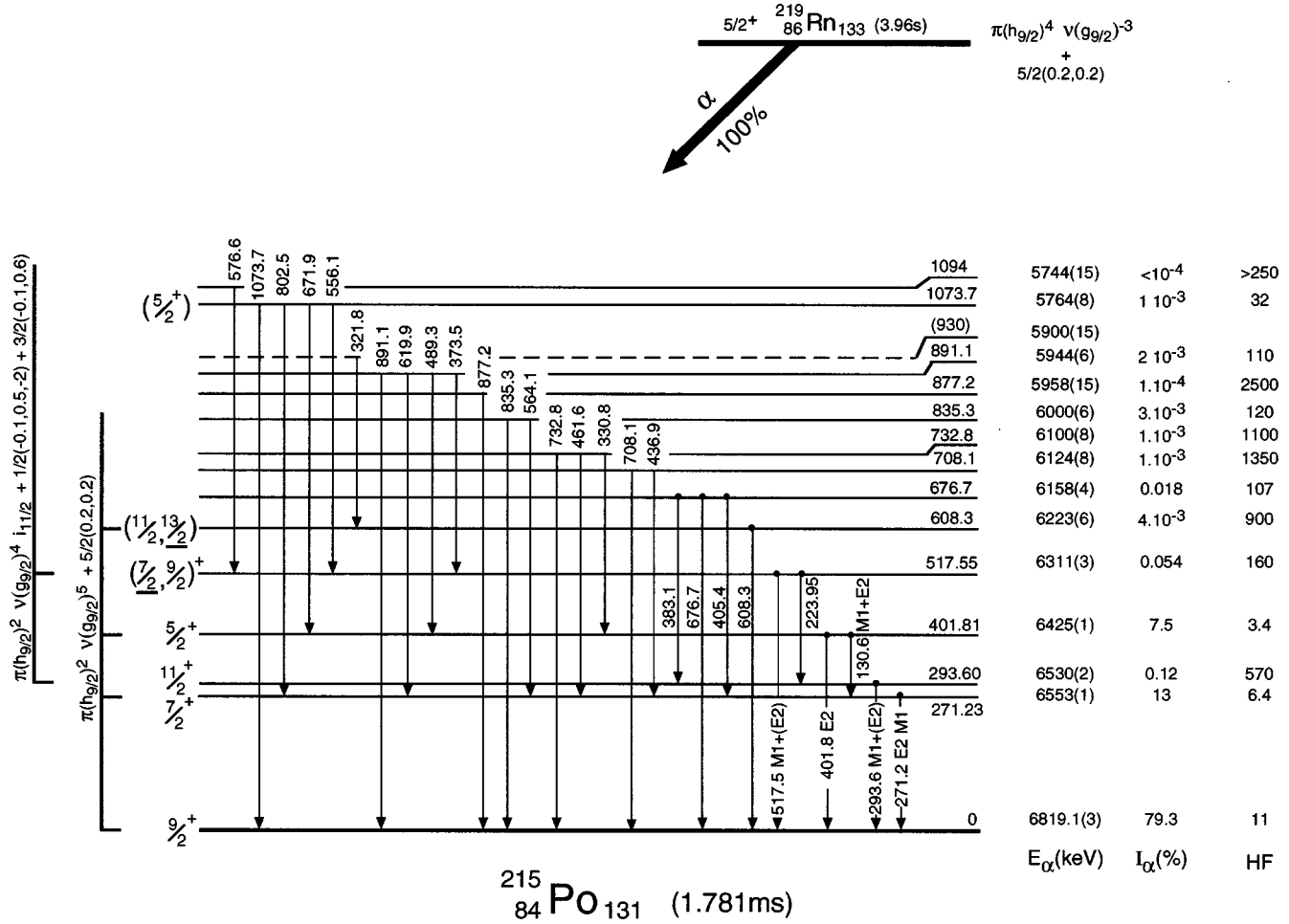

FIG. 5. The level scheme of ^{215}Po following the alpha decay of ^{219}Rn. Transition and level energies are given in keV. Alpha energies, intensities, and hindrance factors (HF's) in the decay of ^{219}Rn are given to the right. Spin assignments are given to the left. Underlined spins are preferred for theoretical reasons (see text). Configurations are indicated.

$19/2^+$, $21/2^+$, and $25/2^+$. When this is coupled with the 0^+, 2^+, 4^+, 6^+, and 8^+ spins arising from the $(h_{9/2})^2$ part of the configuration, a vast number of spins is possible. However, we know that the lowest lying members of the configuration should be $9/2^+$, $7/2^+$, and $5/2^+$ as is observed, for example, in the isotone $^{215}_{86}\mathrm{Rn}_{131}$ [5]. Furthermore, the alpha decaying parent ^{219}Rn with shell model configuration $\pi(h_{9/2})^4\nu(g_{9/2})^{-3}$ and ground state $J^\pi=5/2^+$ would be expected to decay into the $\pi(h_{9/2})^2\nu(g_{9/2})^5$ configuration of ^{215}Po with low HF's. The HF's of 11, 6.4, and 3.4 to the $9/2^+$, $7/2^+$, and $5/2^+$ are exactly what is expected. The next state which might be expected in this configuration is the $13/2^+$ which is very tentatively assigned at 608.3 keV. It decays to the $9/2^+$ ground state only as would be expected for the $13/2^+$ state.

The next configuration expected in ^{215}Po is $\pi(h_{9/2})^2\nu(g_{9/2})^4 i_{11/2}$. The equivalent configuration in the isotone ^{217}Rn has been observed [5] with the spin sequence $11/2^+,7/2^+,3/2^+$. A good candidate for the configuration bandhead is observed at 293.60 keV. It has a HF of 570 in contrast to low HF's of neighboring states, and decays with a single $M1+(E2)$ transition to the $9/2^+$ ground state and is tentatively assigned $J^\pi=(11/2)^+$. The next state expected in this configuration is the $7/2^+$ state. A possible candidate is observed at 517.55 keV. It decays to the $(11/2)^+$ bandhead of the configuration and to the $9/2^+$ ground state with an $M1+(E2)$ transition.

It is possible to make multiple assignments to the remaining states, but since it is not obvious to which configurations they belong, we have not done this. One state which deserves further mention is the state at 1073.7 keV. Its HF=32, much lower than any other state except the $9/2^+$, $7/2^+$, and $5/2^+$ members of the ground state configuration. It seems probable that it belongs to the ground state configuration and we have very tentatively assigned it $J^\pi=(5/2^+)$.

V. DISCUSSION

The nucleus ^{215}Po with just two protons and five neutrons beyond the double closed shell in ^{208}Pb is an obvious candidate for explanation in terms of $g_{9/2}$ and $i_{11/2}$ shell model configurations. These configurations are discussed in Sec. IV of this paper. However, this nucleus is also on the edge of the region of intrinsic reflection asymmetry. It is therefore of interest to see what effect this special symmetry has on ^{215}Po.

Figure 6 presents the parity mixed neutron orbitals [6] appropriate for this transition region. These octupole deformed Nilsson orbitals are calculated with an axially symmetric reflection asymmetric ($\varepsilon_3=0.08$) folded Yukawa po-

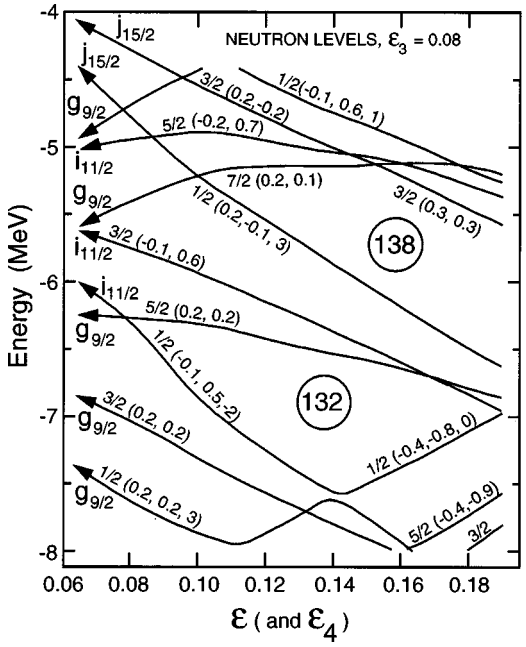

FIG. 6. Parity mixed neutron orbitals calculated in an axially symmetric but reflection asymmetric ($\varepsilon_3 = 0.08$) folded Yukawa potential [6] plotted against quadrupole deformation (ε). See text for more detail.

tential [6]. The levels are labeled by $\Omega(\langle\hat{s}_z\rangle,\langle\hat{\pi}\rangle)$, and in the case of $K=1/2$ orbitals, a third quantum number listed last in the parentheses $\langle\pi_{\rm conj}|-\hat{j}_+|R_{\rm conj}\rangle$. The shell model symbols on the left-hand side of the figure near the arrows are the shell model configurations to which the orbitals will revert when $\varepsilon_2=\varepsilon_3=0$. Using this figure we note that for ^{215}Po the 131st neutron, at the expected very small deformation $\varepsilon \cong 0.07$, will occupy the $g_{9/2}$ shell model orbital with the associated reflection asymmetric orbital 5/2(0.2,0.2) while immediately above is the $i_{11/2}$ orbital associated with the 1/2 $(-0.1,0.5,-2)$ associated reflection asymmetric orbital. These are the ground state and first excited state configurations experimentally observed for ^{215}Po in Sec. IV.

It is now of interest to see if we can understand the spectroscopy as we approach systematically with lower neutron and proton number toward the double closed shell at ^{208}Pb. More specifically, we are interested to see how the reflection asymmetric orbitals of Fig. 6 approach the shell model orbitals in passing through the transition region.

In order to understand the ''band'' structure of the $\pi(h_{9/2})^2\nu(g_{9/2})^5$ ground state configuration of ^{215}Po, it is instructive to compare it with the structure of the $g_{9/2}$ and associated 5/2(0.2,0.2) reflection asymmetric orbital in neighboring nuclei. This comparison with ^{223}Ra [7], ^{221}Ra [8], ^{219}Ra [9], ^{219}Rn [1], and ^{217}Rn [5] is made in Fig. 7. All of the bandheads (either $5/2^+$ or $9/2^+$) in Fig. 7 are assigned an energy of 0 keV to put them on the same footing for the comparison. States with the same spin and positive parity are connected by dashed lines and those bandheads with negative parity, with dotted lines. From left to right the nuclei decrease in mass number and in proton and neutron number as they approach the region of ^{208}Pb.

To the left in Fig. 7 the level structures of ^{223}Ra and ^{221}Ra have quite regular structures of $K=5/2^+$ bands indicative of the 5/2(0.2,0.2) parity mixed orbital of Fig. 6. The $K=5/2^-$ parity doublet bandheads are observed quite low in energy at 134.5 and 103.4 keV, respectively, as expected for a reflection asymmetric nucleus. As we move down in mass

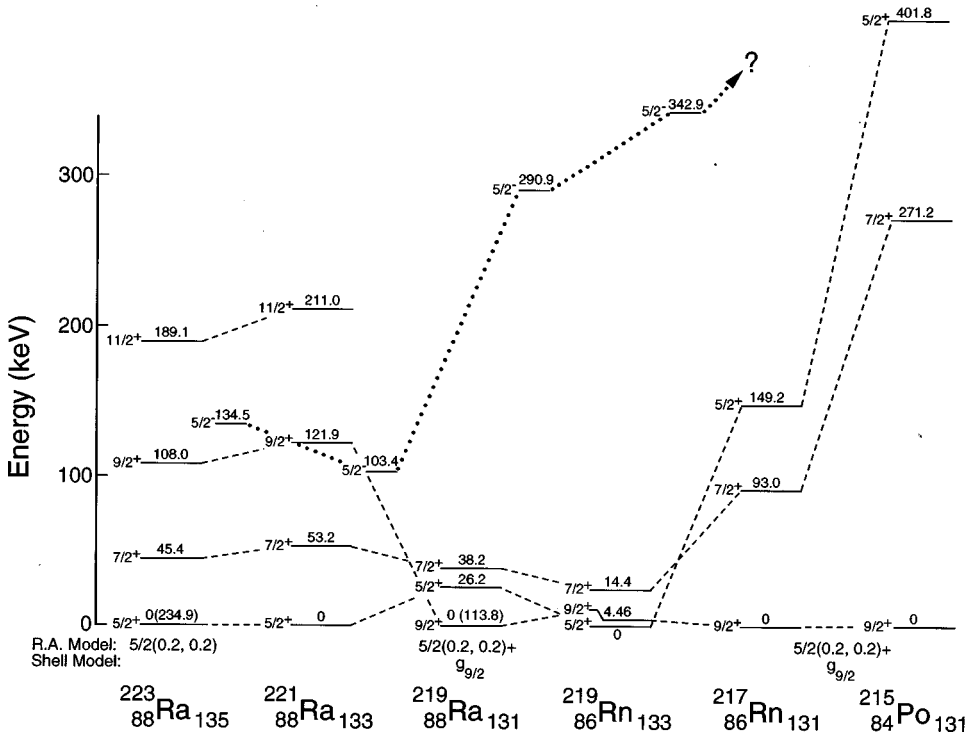

FIG. 7. Comparison of selected level structures of the $K=5/2\pm$ bands of ^{223}Ra, ^{221}Ra, ^{219}Ra, ^{219}Rn, ^{217}Rn, and ^{215}Po. States of the same spin and positive parity are connected by dashed lines. States of the same spin and negative parity are connected by dotted lines. See text for interpretation.

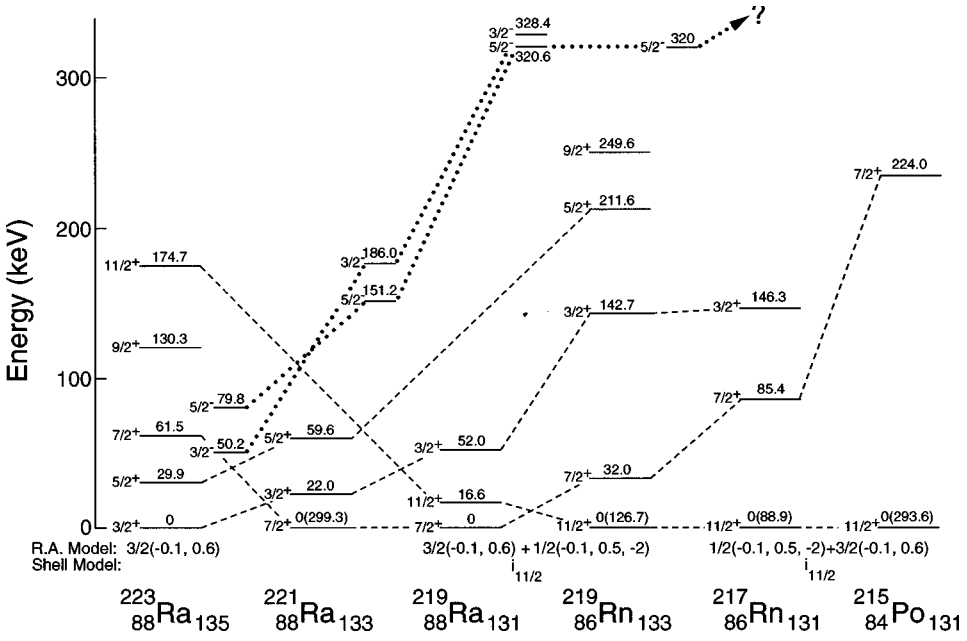

FIG. 8. Comparison of selected levels of the $K=3/2\pm$ bands of ^{223}Ra, ^{221}Ra, ^{219}Ra, ^{219}Rn, ^{217}Rn, and ^{215}Po. States of the same spin and positive parity are connected by dashed lines, those of negative parity by dotted lines. See text for interpretation.

number to ^{219}Ra and ^{219}Rn, it is obvious that drastic alteration of the rotational structure of ^{223}Ra and ^{221}Ra has occurred. The structure is very much compressed and the $9/2^+$ state has become the bandhead in ^{219}Ra and only 4.46 keV above the bandhead in ^{219}Rn. This is obviously indicative of the increasing importance of the $g_{9/2}$ shell model configuration. At the same time, the $K=5/2^-$ parity doublets have moved decisively higher to 290.9 and 342.9 keV in ^{219}Ra and ^{219}Rn, respectively, indicative of the decreasing importance of reflection asymmetry.

Finally when we move to the right in Fig. 7 we see that the $9/2^+$ state has decisively become the ground state in ^{217}Rn and ^{215}Po with a great deal of $g_{9/2}$ shell model character. Nonetheless, the alpha decay HF from the ^{221}Ra $5/2^+$ ground state to the $5/2^+$ state of ^{217}Rn at 149.2 keV is 3 [5], and from the ^{219}Rn $5/2^+$ ground state to the $5/2^+$ state at 401.8 keV in ^{215}Po is 3.4 as observed in this research. These very low HF's suggest that there is still some reflection asymmetric character in ^{217}Rn and ^{215}Po. There is, however, no evidence of the parity doublet $K=5/2^-$ bands in either ^{217}Rn or ^{215}Po. Thus as we move toward ^{208}Pb from higher mass numbers, we go from a $K=5/2^+$ reflection asymmetric spectroscopy to a $K=5/2^+$ mixed reflection asymmetric-$g_{9/2}$ shell model spectroscopy to a dominant but not completely dominant $g_{9/2}$ shell model spectroscopy.

The ''band'' structure of the $\pi(h_{9/2})^2\nu(h_{9/2})^4 i_{11/2}$ configuration in ^{215}Po is compared with the same set of nuclei used in Fig. 7 in Fig. 8. As in Fig. 7 all bands with the same spin and positive parity are connected by dashed lines and all $3/2^-$ and $5/2^-$ bands are connected by dotted lines. The ordering of the nuclei is the same in Figs. 7 and 8.

At the left of Fig. 8, the $K=3/2^+$ band of ^{223}Ra has a reasonably regular rotational structure, although there is evidence that the states of negative simplex quantum number (i.e., $3/2^+$, $7/2^+$, and $11/2^+$) are lowered with respect to states with positive simplex quantum number ($5/2^+$ and $9/2^+$). Moving right in the systematics, the $7/2^+$ state of ^{221}Ra has become the bandhead. It remains the bandhead in ^{219}Ra; however, the $11/2^+$ state has come down all the way to 16.6 keV. In ^{219}Rn the $11/2^+$ state is the bandhead and becomes even more decisively so in ^{217}Rn and ^{215}Po.

The fact that the negative simplex states move down in energy in the $K=3/2^+$ bands results from the Coriolis coupling of the $K=3/2^+$, $3/2(-0.1,0.6)$ band with the $K=1/2^+$, $1/2(-0.1,0.5,-2)$ band (see Fig. 6) and from the approach to spherical symmetry and the $i_{11/2}$ shell model state. These two effects reinforce each other. For example, as we approach spherical symmetry the energy difference between the 1/2 and 3/2 band decreases, the Coriolis coupling constant increases, and the negative decoupling parameter of the $K=1/2$ band becomes more negative. All of these effects cause the negative simplex states to move down in energy until the normal band structure is destroyed and the $11/2^+$ state becomes the bandhead and finally the $i_{11/2}$ shell model state. These effects are obvious in Fig. 8. The $K=3/2^-$ parity doublet partner increases in energy from 50 keV in ^{223}Ra to 320 keV in ^{219}Ra and ^{219}Rn. This suggests that the octupole collectivity is decreasing. It is also interesting that just as the negative simplex states are lowered for the $3/2^+$ band, the positive simplex states are lowered for the $3/2^-$ parity doublet band. This is indicated in Fig. 8 by the reversal in order of the $3/2^-$ and $5/2^-$ states in ^{221}Ra and ^{219}Ra and is expected since the parity doublet $1/2^-$ band will have positive decoupling parameters.

VI. CONCLUSIONS

The level structure of ^{215}Po has been studied using the alpha decay of ^{219}Rn together with the coincident gamma rays and electrons. A total of 14 new gamma ray transitions is observed. The level scheme which had previously resulted from the synthesis of the data [2,3] up through the 676.7 keV level is confirmed in this experiment. Above this energy we observed new levels at 708.1, 877.2, 1073.7, 1094, and pos-

sibly 930 keV, but do not observe the level at 1056 keV or the tentative level at 683.7 keV.

In the lower energy region of the ^{215}Po level structure, some additional tentative spins and parities have been assigned. Of particular interest in this lower energy range is the presence of some states populated by low HF's and others with much higher HF's. This in turn has made it possible to assign the configuration $\pi(h_{9/2})^2\nu(g_{9/2})^5$ with the residual component of the 5/2(0.2,0.2) reflection asymmetric configuration to states populated with low HF's, and the configuration $\pi(h_{9/2})^2\nu(g_{9/2})^4 i_{11/2}$ with residual components of the $1/2(-0.1,0.2,-2)+3/2(-0.1,0.6)$ reflection asymmetric configurations to states populated with high HF's.

In order to sort out the anomalies in the band structures, the systematics of the bands arising from the 5/2(0.2,0.2), $3/2(-0.1,0.6)$, and $1/2(-0.1,0.5,-2)$ reflection asymmetric orbitals is studied in ^{223}Ra, ^{221}Ra, ^{219}Ra, ^{219}Rn, ^{217}Rn, and ^{215}Po. In this way it is possible to see the collapse of the reflection asymmetric orbital configurations into the less degenerate $g_{9/2}$ and $i_{11/2}$ shell model configurations.

One of us (R.K.S.) wishes to thank the hospitality of the CSNSM and the IPN at the Université de Paris-Sud, Campus Orsay.

[1] R. K. Sheline, C. F. Liang, and P. Paris, Phys. Rev. C **57**, 104 (1998).
[2] R. B. Firestone, V. S. Shirley, C. M. Baglin, S. Y. Frank Chu, and J. Zipkin, *Table of Isotopes*, 8th ed. (Wiley, New York, 1996), Vol. 2.
[3] E. Ruchowska, J. Zylicz, C. F. Liang, P. Paris, and Ch. Briançon, J. Phys. G **16**, 255 (1990).
[4] P. Paris, C. F. Liang, and B. Legrand, Nucl. Instrum. Methods Phys. Res. A **357**, 398 (1995).
[5] C. F. Liang, P. Paris, and R. K. Sheline, Phys. Rev. C **55**, 2768 (1997).
[6] G. A. Leander and R. K. Sheline, Nucl. Phys. **A413**, 375 (1984).
[7] R. K. Sheline, Phys. Lett. **166B**, 269 (1986); R. K. Sheline, G. A. Leander, and Y. S. Chen, Nucl. Phys. **A486**, 306 (1988).
[8] C. F. Liang, P. Paris, Ch. Briançon, and R. K. Sheline, Int. J. Mod. Phys. A **5**, 1551 (1990).
[9] R. K. Sheline, C. F. Liang, and P. Paris, Czech. J. Phys. **43**, 603 (1993).